Agricultural Water Management 278 (2023) 108124

Contents lists available at ScienceDirect

Agricultural Water Management

journal homepage: www.elsevier.com/locate/agwat

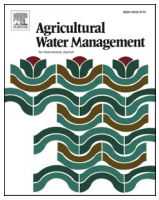

Assessing the biophysical factors affecting irrigation performance in rice cultivation using remote sensing derived information

Alidou Sawadogo [a,*], Elliott R. Dossou-Yovo [b], Louis Kouadio [c], Sander J. Zwart [d], Farid Traoré [e], Kemal S. Gündoğdu [a]

[a] Biosystems Engineering Department, Faculty of Agriculture, University of Uludag, Görükle Kampüsü, 16059 Nilüfer, Bursa, Turkey
[b] Africa Rice Center (AfricaRice), 01 B.P. 2551, Bouake 01, Cote d'Ivoire
[c] Center for Applied Climate Sciences, University of Southern Queensland, West Street, Toowoomba, Queensland 4350, Australia
[d] International Water Management Institute (IWMI), PMB CT 112, Cantonments, Accra, Ghana
[e] Institut de l'Environnement et de Recherches Agricoles, Guisga Street, P.O. Box 8645, Ouagadougou 04, Burkina Faso

ARTICLE INFO

Keywords:
Irrigation performance
Soil property
Machine learning
Surface Energy Balance Algorithm for Land (SEBAL)
Sustainable agriculture
Sub-Sahara Africa

ABSTRACT

Identifying the biophysical factors that affect the performance of irrigated crops in semi-arid conditions is pivotal to the success of profitable and sustainable agriculture under variable climate conditions. In this study, soil physical and chemical variables and plots characteristics were used through linear mixed and random forest-based modeling to evaluate the determinants of actual evapotranspiration (ET_a) and crop water productivity (CWP) in rice in the Kou Valley irrigated scheme in Burkina Faso. Multi-temporal Landsat images were used within the Python module for the Surface Energy Balance Algorithm for Land model to calculate rice ET_a and CWP during the dry seasons of 2013 and 2014. Results showed noticeable spatial variations in PySEBAL-derived ET_a and CWP in farmers' fields during the study period. The distance between plot and irrigation scheme inlet (D_{PSI}), plot elevation, sand and silt contents, soil total nitrogen, soil extractable potassium and zinc were the main factors affecting variabilities in ET_a and CWP in the farmers' fields, with D_{PSI} being the top explanatory variable. There was generally a positive association, up to a given threshold, between ET_a and D_{PSI}, sand and silt contents and soil extractable zinc. For CWP the association patterns for the top six predictors were all non-monotonic; that is a mix of increasing and decreasing associations of a given predictor to either an increase or a decrease in CWP. Our results indicate that improving irrigated rice performance in the Kou Valley irrigation scheme would require growing more rice at lower altitudes (e.g. < 300 m above sea level) and closer to the scheme inlet, in conjunction with a good management of nutrients such as nitrogen and potassium through fertilization.

1. Introduction

Worldwide, more than 70% of the global freshwater resources are used for agricultural production (UNDESAPD, 2014; UN-Water, 2018). In 2018, over 338.7 million ha of agricultural land areas were equipped with irrigation infrastructures in the world, and 15.9 million ha in Africa (FAO, 2020). In most of the countries in Sub-Sahara Africa (SSA), especially those located in the Sahelian zone, the increasing year-to-year rainfall variability (Lebel and Ali, 2009; Paturel et al., 2010), coupled with rapid socioeconomic growth and increasing demand of water for non-agricultural purposes (e.g. urbanization, industrialization), has put substantial pressure on available water for irrigation, thereby worsening water scarcity-related issues in those regions. In countries where agricultural production is predominantly rainfed and farmers are typically subsistence farmers, the recourse to irrigation is crucial to face the adverse effects of rainfall variability and maintain satisfactory yield levels over years to ensure farm profitability and improve farmers' livelihoods. Furthermore, increasing water use efficiency through improved crop water productivity has gained attention over the past years, as emphasized by the United Nations Sustainable Development Goals (SDGs) SGD2.3 and SGD6.4 which refer to the substantial increase in agricultural productivity and water use efficiency by 2030 (Anon, 2015; https://sdgs.un.org/goals). Thus, besides the good knowledge of water available for irrigation over time and of the proportion of irrigated land areas, implementing relevant policies to improve agricultural irrigation water management and achieve the sustainable management of

* Corresponding author.
E-mail addresses: sawadogoalidou@yahoo.fr, alidousawadogo@uludag.edu.tr (A. Sawadogo).

https://doi.org/10.1016/j.agwat.2022.108124
Received 10 January 2021; Received in revised form 18 December 2022; Accepted 21 December 2022
Available online 9 January 2023

irrigated land areas requires a good diagnostic of irrigation performance of these areas and a clear characterization of the environmental factors affecting the performance of irrigated schemes (Bastiaanssen and Bos, 1999; Bos et al., 2005).

Various approaches including field campaigns and surveys, remote sensing (RS)-based methods, are being applied to characterize the performance of irrigated areas temporally and spatially, from field to national scales. Field campaigns and surveys are typically costly, labor-intensive, and time-consuming when dealing with large land areas. On the other hand, RS-based methods can be cost-effective and less time-consuming as remotely sensed data used for assessing the irrigation performance of irrigation schemes are most often readily available and provide continual spatial coverage at frequent time intervals across varying spatial scales (Bastiaanssen and Bos, 1999; Blatchford et al., 2019). Using remotely sensed data also enables the integration of such information with other sources of spatial data (Sheffield and Morse-McNabb, 2015). RS-based approaches have been successfully applied to benchmarking irrigation systems and evaluating various irrigation performance indicators (e.g. equity, adequacy, reliability, productivity) under a variety of climatic conditions and locations worldwide (e.g. Zwart and Bastiaanssen, 2007; Ahmad et al., 2009; Zwart and Leclert, 2010; Kharrou et al., 2013; Sawadogo et al., 2020b). For example, Zwart and Bastiaanssen (2007) quantified the spatial variation of evapotranspiration (ET_a), crop yield, and crop water productivity (CWP) in irrigated wheat systems in different countries including Pakistan, China, Egypt, India, the Netherlands, Mexico, and the U.S.A., using the Surface Energy Balance Algorithm for Land (SEBAL; Bastiaanssen and Ali, 2003; Bastiaanssen et al., 2005) and satellite images from the National Oceanic and Atmospheric Administration-Advanced Very High Resolution Radiometer (NOAA-AVHRR) and Landsat satellite sensors. Kharrou et al. (2013) investigated the variability in irrigation performance of an irrigated scheme in central Morocco, consisting mainly of wheat fields and olive orchards, using RS satellite-derived indicators (i.e. relative irrigation supply, depleted fraction, relative evapotranspiration, and the coefficient of variation of crop evapotranspiration). Recently, Sawadogo et al. (2020b) investigated the irrigation performance of the Kou Valley irrigation scheme (KVIS), Burkina Faso, using the python module for SEBAL (PySEBAL) and Landsat-7 ETM+ and Landsat-8 Operational Land Imager (OLI) / Thermal Infrared Sensor (TIRS) satellite images. The KVIS is a 1200-ha irrigation scheme characterized by a diversity of crops, including cereals, tubers, and vegetables (DRASA-Ouest, 2014). The authors found a gradient of spatially varying relative evapotranspiration across the KVIS, resulting in four main crop areas according to the degree of water stress and associated variable crop water productivity for rice, sweet potato and maize (Sawadogo et al., 2020b). The authors suggested that such variability can be explained by various factors including the number of upstream water users and soil types and properties (Sawadogo et al., 2020b).

The variation of irrigation performance across a given irrigation scheme can be attributed to several factors including rainfall variability, soil physical properties, soil fertility, topography, and crop management practices (Bastiaanssen and Steduto, 2017; Foley et al., 2020). This study builds upon Sawadogo et al. (2020b) and aims at investigating plot characteristics and soil physicochemical properties affecting irrigation performance in rice cropping across the KVIS, using RS-derived data and irrigation performance indicators. In countries like Burkina Faso where reliable and readily available long-term observed data of soil properties are limited, such RS-derived data hold the potential for addressing such research questions. The use of satellite RS data to obtain spatial and multitemporal soil properties data has been extensively documented in the literature (e.g. Chang and Islam, 2000; Ge et al., 2011; Forkuor et al., 2017; Fontanet et al., 2018; Yuzugullu et al., 2020). Satellite-derived soil data have been used within traditional (e.g. generalized linear and logistic models) and machine learning (e.g. artificial neural networks, random forest (RF), boosted regression tree-based models) modeling frameworks for various purposes in agriculture including land use suitability (e.g. Laborte et al., 2012; Akpoti et al., 2020; Akpoti et al., 2022), assessment of irrigation status according to crop type (e.g. Mohamed et al., 2019), and the assessment of drought predictors in inland valley rice-based production systems (e.g. Dossou-Yovo et al., 2019). In this study, linear mixed and RF-based models were employed to assess the main soil physical and chemical variables and plot characteristics (i.e. distance to the inlet scheme and elevation) that explain the variabilities in ET_a and CWP in rice (*Oryza glaberrima*) cultivation across the KVIS during the dry season production periods in 2013 and 2014. This research contributes to improved management of irrigation water as supported by satellite remote sensing. It aims at identifying the main soil physical and chemical properties and plot attributes affecting the spatial variation of irrigation performance across the KVIS. Such identification could serve as basis for implementing strategies for a better management of the spatial constraints of crop production in irrigation schemes in Burkina Faso and regions with similar environmental conditions.

2. Materials and methods

2.1. Study area

The Kou Valley irrigation scheme is a river-diversion irrigation scheme divided into eight blocks (Fig. 1), which is located in the Kou watershed, a relatively water-rich watershed in southwest Burkina Faso (Wellens et al., 2013). With alternate rainy (June to September) and dry (October to May) seasons, the Kou watershed is characterized by a sub-humid climate (Wellens et al., 2004; Traoré, 2012), with annual rainfall varying between 900 mm and 1100 mm and potential evapotranspiration up to 2000 mm on average (Dembélé et al., 2012; Traoré, 2012). The monthly minimum and maximum temperatures are on average 18 °C and 37 °C, respectively; and the relative humidity ranges from 20% to 80% annually (Traoré, 2012). The KVIS diverts water from the Kou river into its irrigation canals at an average flow rate of 3.5 $m^3 s^{-1}$ and 1.4 $m^3 s^{-1}$ during the rainy and dry seasons, respectively (Wellens et al., 2013).

Six dominant soil types are found across the KVIS: clay, clay loam, sandy clay, sandy clay loam, loam, and sandy loam (Dembélé et al., 2012). Plot size in the KVIS varies between 0.2 ha and 1.5 ha. Irrigation water is typically supplied through the basin system, with the critical period of irrigation spanning from January to April. Rice nursery most often starts in December followed by transplantation in January. The growth cycle varies between 90 and 120 days, with harvest occurring in May. During the study period (2013 and 2014) New Rice for Africa (NERICA) cultivars were sown across the KVIS by farmers, with the areas sown being 452 ha and 317 ha in 2013 and 2014, respectively (Nitcheu et al., 2014). Potential paddy yields for rice cultivars sown during the study period ranged from 5.0 to 7.0 t ha^{-1} (Nitcheu et al., 2014).

2.2. Data

2.2.1. Biophysical predictors data

Various soil physicochemical variables, sourced from the Africa Soil Information Service (AfSIS; Hengl et al., 2015) and the Africa Soil Profiles database compiled for AfSIS (ISRIC, 2014), were used as potential explanatory variables in this study. There were: depth to bedrock (DtB), bulk density (BLD), clay content (CL), silt content (SL), sand content (SN), soil organic carbon (SOC), available water capacity (AWC), potential of hydrogen (pH), cation exchange capacity (CEC), total nitrogen (N), and extractable calcium (Ca), iron (Fe), magnesium (Mg), phosphorus (P), potassium (K), and zinc (Zn). Except for the depth to the bedrock, soil physicochemical properties were extracted for the topsoil layer of 30 cm due to the shallow rooting depth of rice plants. Soil physicochemical variables from the AfSIS and the Africa Soil Profiles database compiled for AfSIS represent an average status of soil

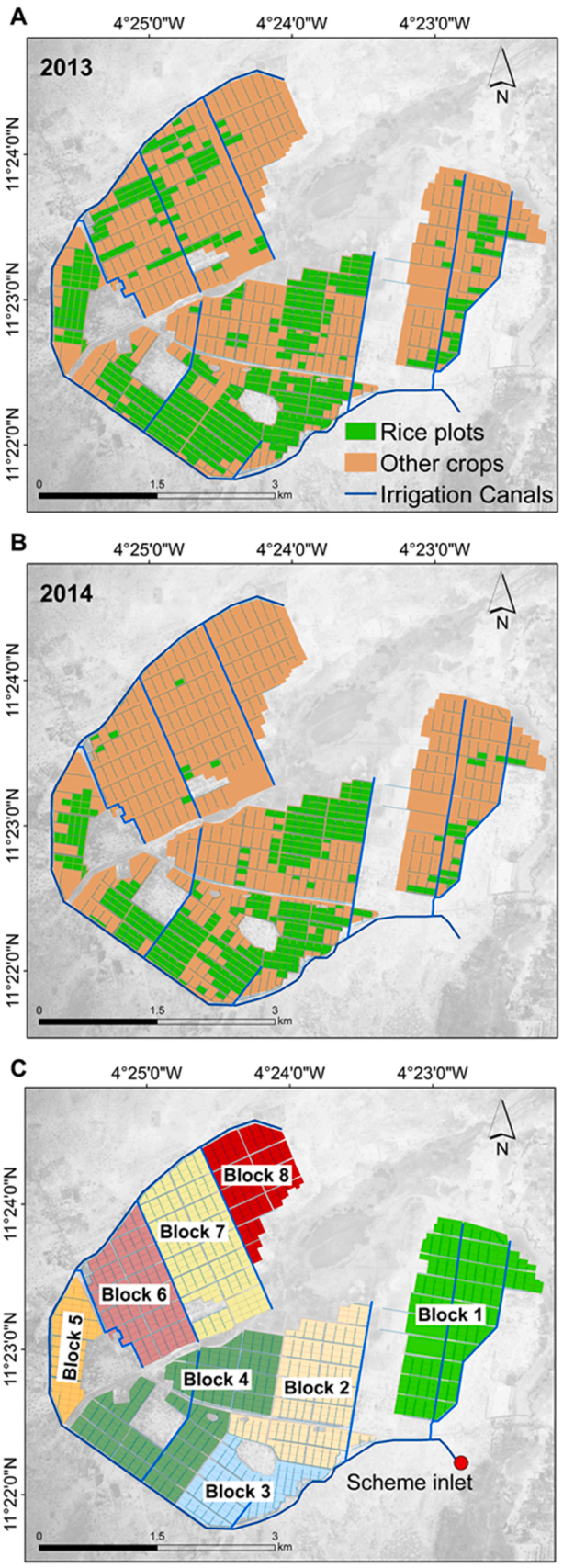

Fig. 1. Rice plots during the dry season in 2013 (**A**) and 2014 (**B**), and distribution of irrigation canals and blocks (**C**), at the Kou Valley irrigation scheme in Burkina Faso. The scheme inlet is represented by a red dot in (**C**).

properties at 250-m spatial resolution, encompassing the 1960–2016 period (Hengl et al., 2015, 2017). Such soil properties data have proven effective in understanding the sources of variation in several crop fields, including rice, in SSA (Djagba et al., 2018; Dossou-Yovo et al., 2019; Akpoti et al., 2020). Further information on the methodology of soil data compilation and assessment of soil nutrient maps in the AfSIS can be found in Leenaars et al. (2014), Hengl et al. (2015, 2017).

Two additional variables related to each of the rice plots were included in the analysis: the plot's elevation and the distance between the plot and the scheme inlet (D_{PSI}). Plot elevations were extracted from the 30-m spatial resolution digital elevation model, sourced from the U. S. National Aeronautics and Space Administration (NASA)'s Shuttle Radar Topography Mission (Farr et al., 2007). D_{PSI} was determined as the sum of distances between the centroid of each rice plot and the nearest secondary canal inlet, and between that secondary canal inlet and the main scheme inlet of the KVIS, using the near distance tool from the ArcGIS software.

2.2.2. PySEBAL-derived actual evapotranspiration and crop water productivity

Multi-temporal clear-sky satellite images from Landsat-7 ETM+ and Landsat-8 OLI/TIRS, retrieved from the website https://earthexplorer.usgs.gov/, and spanning the study period were used within PySEBAL to estimate ET_a and CWP for rice at a 30-m spatial resolution. Additional input data in PySEBAL included hourly and daily weather data (average air temperature, wind speed, relative humidity, and solar radiation) and digital elevation model data. ET_a values were derived as residuals of the surface energy balance. CWP was determined as the ratio between yield and ET_a, both estimated using PySEBAL. Rice yield was estimated as follows:

$$Yield = \frac{Biomass \times HI}{1 - Moist} \quad (1)$$

where *Biomass* is the crop biomass estimated using PySEBAL (kg ha^{-1}); *HI* refers to the harvest index (0.45 in this study); and *Moist* is the moisture content of the grain at harvest (17% in this study).

Biomass values in PySEBAL are estimated as a function of the fraction of absorbed photosynthetically active radiation, and light use efficiency (Bastiaanssen and Ali, 2003). The value for *HI* in this study was selected based on reported values in the literature (Steduto et al., 2012); *Moist* value was from the average moisture contents observed at the KVIS (Nitcheu et al., 2014). A full description of the calculation methods of ET_a and CWP using PySEBAL, as well as performance results of PySEBAL in estimating ET_a across the KVIS can be found in Sawadogo et al. (2020a) and Sawadogo et al. (2020b). Comparisons between the FAO Water Productivity through Open access of Remotely sensed derived data (FAO-WaPOR) and PySEBAL-derived ET_a values indicated that PySEBAL satisfactorily estimated ET_a values across the KVIS, with R^2 and root mean square error (RMSE) values ranging from 0.74 to 0.80 and 3.6–11.0 mm, respectively, for the dekadal estimates, while for the seasonal estimates of ET_a the corresponding values were 0.60–0.70 and from 64 mm to 150 mm, respectively (Sawadogo et al., 2020b).

In this study, pixel values from the AfSIS and the Africa Soil Profiles database compiled for AfSIS (both at 250-m spatial resolution) were extracted for each of the rice plots using QGIS (version 2.18.27; https://qgis.org/). For a rice plot overlapping two pixels, the average value of pixels was considered. All maps were plotted using ArcGIS (version 10.4; ESRI, 2016).

2.3. Data analysis

2.3.1. Linear mixed model (LMM)

The formula for the linear mixed model (LMM) used in the study is as follows (Laird and Ware, 1982; Peng and Lu, 2012):

$$Y = X\beta + Zu + \varepsilon \quad (2)$$

where Y is a $N \times 1$ column vector of the outcome variable (ET_a or CWP in this study). $N = 770$; X is a $N \times p$ matrix of the predictors; β is a $p \times 1$ column vector of the fixed-effect regression coefficients; Z is a $N \times qJ$ design matrix for the q random effects and J groups; u is a $qJ \times 1$ vector of q random effects (the random complement of the fixed β) for J groups; and ε is a $N \times 1$ column vector of the residuals. β is distributed as a random normal variable with mean μ and standard deviation σ; that is in equation form $\beta \sim N(\mu, \sigma)$.

In the LMM, the response variables were ET_a or CWP (both obtained with PySEBAL); KVIS blocks were used as random effect factors; and soil physicochemical characteristics and plot attributes were considered as fixed effect factors. The original dataset was randomly divided into 70% and 30% for training and testing, respectively. The training dataset was used for testing the significance of the fixed effects (significance level $\alpha = 0.05$). The goodness-of-model-fit was assessed using the testing dataset. To avoid multi-collinearity, explanatory variables with correlation coefficient ≥ 0.75 were removed beforehand. Only one of the strongly correlated variables was kept for the subsequent analyses. Additionally, all data were standardized [mean(x)/2 ×sd(x)] to allow for direct comparison of effect sizes (Gelman and Hill, 2007). The relative importance of each predictor was assessed through the general dominance analysis (Azen and Budescu, 2003; Luo and Azen, 2013), using the package 'dominanceanalysis' (Bustos-Navarrete and Filipa, 2020). The Nakagawa's marginal R^2 (Nakagawa and Schielzeth, 2013) was used as statistical indicator for comparing the relative importance of predictor in the dominance analysis. All LMM calculations were carried out using the packages 'nlme' (Pinheiro et al., 2020) and 'lme4' (Bates et al., 2015) in R (version 4.0.0; R Core Team, 2020).

2.3.2. Random forest-based (RF) model

Random forests are based on a learning algorithm relying on the concept of model aggregation (Breiman, 2001; Prasad et al., 2006). They combine binary decision trees built with bootstrapped samples from the learning sample where a subset of predictors has been chosen randomly at each node (Prasad et al., 2006; Kouadio et al., 2018). RF was used to estimate the importance of the potential predictors (or explanatory variables) of ET_a or CWP in rice plots across the KVIS.

The same randomly divided datasets used for training and testing in the LMM approach were used. The number of decision trees (*Ntree*) was set to 500. The optimal minimum number of observations per tree leaf (*mtry*) was selected automatically during the execution of the RF algorithm, using the 'caret' package (Kuhn et al., 2020). Variable importance, partial dependence plot and model prediction were used as tools for evaluating the performance of the RF-based models. The training dataset was used for both variable importance and partial dependence plot analyses, whereas the testing dataset was used for analyzing model prediction. The mean decrease accuracy was used as a measure of variable importance, which was based on the regression prediction error of the out-of-bag (OOB) data (Breiman, 2001; Liaw and Wiener, 2002). Mean decrease accuracy was calculated as the normalized difference between the OOB accuracy of original observations and that of randomly permuted variables (Cutler et al., 2007; Mellor et al., 2013). The partial dependence plot analysis shows the isolated effect of the chosen predicator variable on the response variable (Friedman, 2001). Only the top six important explanatory variables were used for the partial dependence plot analysis in this study. Model prediction analysis was carried out using the '*predict*' method for RF objects from the 'randomForest' package (Liaw and Wiener, 2018) in R (version 4.0.0; R Core Team, 2020).

2.3.3. Model evaluation

The coefficient of determination (R^2), the Nash–Sutcliffe efficiency index (NSE; Krause et al., 2005), and the root mean square error (RMSE) were used to assess the goodness-of-fit of the LMM and RF models and compare their performance. The formulas for R^2, NSE, and RMSE are as follows:

$$R^2 = \frac{\sum_{i=1}^{n}(O_i - \overline{O}).(P_i - \overline{P})}{\sqrt{\sum_{i=1}^{n}(O_i - \overline{O})^2.\sum_{i=1}^{n}(P_i - \overline{P})^2}} \quad (3)$$

$$NSE = 1 - \frac{\sum_{i=1}^{n}(O_i - P_i)^2}{\sum_{i=1}^{n}(O_i - \overline{O})^2} \quad (4)$$

$$RMSE = \sqrt{\frac{1}{n}\sum_{i=1}^{n}(P_i - O_i)^2} \quad (5)$$

where P_i and O_i refer to the predicted and PySEBAL-derived values of ET_a or CWP, respectively; $\overline{P}$ and $\overline{O}$ are the average predicted and PySEBAL-derived values of ET_a or CWP, respectively; and n is the testing sample number.

Lower RMSE values and R^2 or NSE values close to 1 are indicative of good model performance.

3. Results

3.1. Rice growing environment, actual evapotranspiration and water productivity

A correlation matrix for each pair of the potential explanatory variables is shown in Fig. S1. From the initial set of variables, only 12 were considered in the modeling. These were: D_{PSI}, Elv, DtB, BLD, SL, SN, pH, N, Ca, Fe, K, and Zn. Noticeable variations in these soil properties were found across the KVIS (Table 1; Fig. S2). Compared to the other chemical elements, Ca was dominant in the 0–30 cm soil horizon: its proportion ranged from 581 to 1427 ppm, with an average of 885 ppm (Table 1). Values of pH varied between 5.9 and 6.4, indicating that rice was grown on acidic soils during the study period. The range of pH found for rice plots across the KVIS was within the correct balance of soil pH for rice (5.5 and 7.5; Yu, 1991; Nishikawa et al., 2014). The DtB was on average 157 cm, with the maximum being 174 cm. Sand and silt proportions at 15–30 cm depth varied between 38 and 49 w% and 23 and 31 w%, respectively; suggesting that at this depth the soils of rice plots were more sandy clay to sandy clay loam. Rice plots were located at 295–310 m above sea level (masl) (Table 1), with the majority of plots (> 75%) being above 300 masl. The closest plot to the KVIS scheme inlet was at 815 m, and the farthest was at 11,289 m (Table 1). Large variations were found in the soil physico-chemical properties, plot elevation and distance to the inlet of the irrigation scheme in farmers' fields

Table 1
Descriptive statistics of the physical characteristics of rice plots across the Kou valley irrigation scheme.

Variables[a]	Units	Mean	CV[b]	Min	Max
Plot characteristics					
Elv	m	302	0.97	295	310
D_{PSI}	m	4807	49.1	815	11,289
Soil physico-chemical properties					
DtB	cm	157	4.12	141	174
BLD	kg m^{-3}	1355	3.31	1300	1650
SL	w%	26	5.06	23	31
SN	w%	42	4.64	38	49
Ca	ppm	885	19.4	581	1427
Fe	ppm	133	7.32	109	151
K	ppm	122.6	11.1	94	157
N	ppm	770	7.01	584	879
pH	–	6.2	1.44	5.9	6.4
Zn	pp100m	240	10.56	155	384

[a] Elv: plot elevation; DPSI: distance between plot and irrigation scheme inlet; DtB: depth to bedrock; BLD: bulk density; SL: silt content; SN: sand content; Ca: soil extractable calcium; Fe: soil extractable iron; K: soil extractable potassium; N: soil total nitrogen; pH: potential of hydrogen; Zn: soil extractable zinc.
[b] CV: Coefficient of Variation.

(Table 1).

With regard to estimated rice ET_a, relatively higher values were found in 2014 compared to those in 2013, with the averages being 619 mm (range = 239–794 mm) and 554 mm (range = 178–750 mm), respectively (Fig. 2A). Estimated water productivity values were on average 0.53 kg m^{-3} (range = 0.15–1.09 kg m^{-3}) and 0.59 kg m^{-3} (range = 0.31–1.30 kg m^{-3}) in 2013 and 2014, respectively (Fig. 2B).

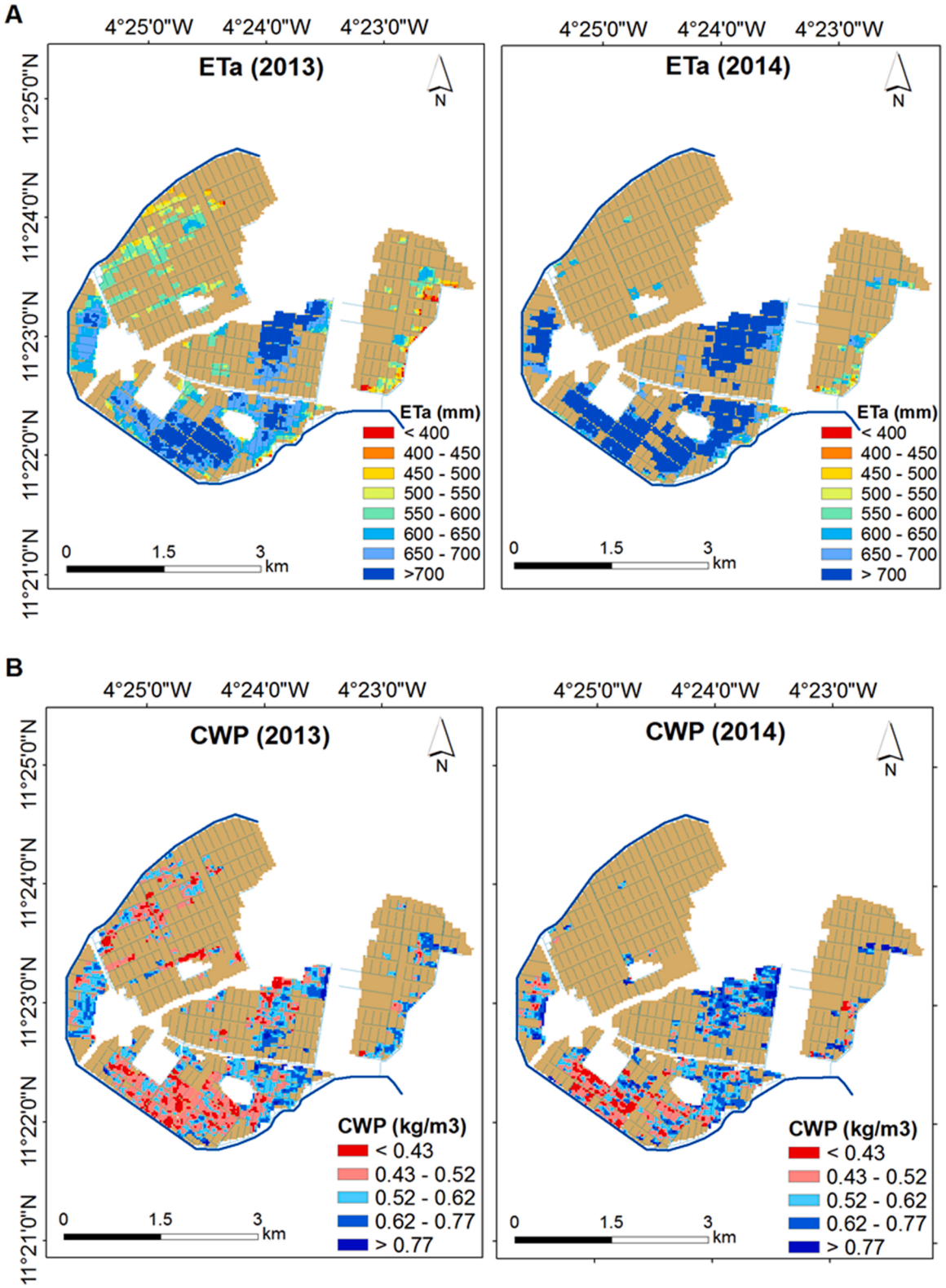

Fig. 2. Spatial variation of (**A**) PySEBAL-derived seasonal actual evapotranspiration (ET_a) and (**B**) PySEBAL-derived crop water productivity (CWP) in rice plots across the Kou Valley irrigation scheme during the dry season production periods in 2013 and 2014. Plots in brown are cropped with other crops.

3.2. Determinants of actual evapotranspiration and crop water productivity

3.2.1. Assessment using linear mixed modeling approach

Table 2 shows the estimates of each of the predictors, as well as their statistical significance. Overall, the distance between plot and irrigation scheme inlet (D_{PSI}), depth to bedrock (DtB), bulk density (BLD), silt content (SL), sand content (SN), total soil nitrogen (N) and potassium (K), were the predictors explaining the variability in rice ET_a ($p < 0.05$; Table 2). Factors such as D_{PSI}, BLD, SL and SN were negatively related to ET_a. Thus, the farther the rice plot was from the scheme inlet, the lower its ET_a was. Likewise, the higher the soil content in silt or sand or the bulk density, the lower the ET_a. Other statistically significant predictors, DtB, N and K, were positively related to ET_a (Table 2). On the other hand, there were fewer predictors that affected significantly rice CWP during the study period. These predictors were plot elevation (Elv), D_{PSI}, and N (Table 2). All these three predictors were negatively related to CWP, indicating that low CWP occurred either in rice plots located at higher altitudes, or in plots far from the inlet scheme, or in plots with soils having relatively higher N concentrations.

The results of the general dominance analysis for ET_a and CWP are presented in Fig. 3. For the variability in ET_a, D_{PSI} and N were the predictors with relatively higher marginal R^2 values: 0.165 and 0.125, respectively (Fig. 3A). The marginal R^2 for the other statistically significant predictors (BLD, DtB, SL, SN, K; Table 2) varied between 0.010 and 0.020 (Fig. 3A). For CWP, D_{PSI} had the highest marginal R^2 value (0.107; Fig. 3B). The remainder of the statistically significant predictors (Elv, N) had their marginal R^2 ranging from 0.010 to 0.030 (Fig. 3B).

3.2.2. Assessment using random forest-based modeling approach

Overall, the rank of each of the variables based on the RF models differed according to the response variables (Fig. 4). Exception included the variable D_{PSI}, which was found to contribute the most in both rice ET_a and CWP with 52% and 22% for the mean decrease in accuracy, respectively (Fig. 4). For rice ET_a, besides D_{PSI}, variables with contribution $>$ 20% included extractable zinc (Zn), potassium (K) and N (Fig. 4A). Silt and sand contents, and bulk density contributed to about 11–16%, respectively. The top six contributors were D_{PSI}, N, Zn, K, SN, and SL (Fig. 4A). For rice CWP, the majority of the remaining 11 explanatory variables had their contribution to the RF-based model varying between 10% and 20%; DtB and BLD were the less-contributing predictors ($\leq$ 7%) (Fig. 4B). The top six contributors, based on the RF approach, were D_{PSI}, K, N, Elv, Ca, and SN (Fig. 4B).

Figs. 5 and 6 show the partial dependence plots for the top six predictors explaining variabilities in rice ET_a and CWP, respectively. They displayed the pattern of association (i.e. monotonic or non-monotonic, linear or non-linear) between the predictor and the response variable. Among the top six covariates, only the relationship between rice ET_a and K or N was monotonic: an increase in K or N concentration was positively associated to an increase in rice ET_a, with that of K being linear (Fig. 5). Non-monotonic associations were found between rice ET_a and D_{PSI}, Zn, SN and SL (Fig. 5). For those predictors, there was generally an increasing trend to rice ET_a up to a given threshold, followed by a decreasing trend (Fig. 5).

With regard to rice CWP, the association patterns for the top six predictors were all non-monotonic (Fig. 6). That is, there was a mixed of increasing and decreasing associations of a given predictor to either increasing or decreasing CWP, depending on predictor value. For example, for plot elevation and soil total nitrogen (N), there was a decreasing association to rice CWP up to a given threshold value of the predictor (i.e. 305 m for Elv, and 780 ppm for N), before an increasing association afterwards (Fig. 6).

3.3. Comparison of LMM and RF-based models performance

Both LMM and RF-based models achieved good performance in predicting ET_a: RMSE were 39 mm and 38 mm, respectively; their corresponding R^2 being 0.74 and 0.75 and NSE being 0.74 and 0.75 (Fig. 7A). However, for CWP the performance of both models was fair: RMSE $= 0.07$ kg m^{-3} and 0.08 kg m^{-3} for RF-based model and LMM, respectively; corresponding R^2 of 0.43 and 0.38, respectively (Fig. 7B). This suggests that additional observational data are needed for better assessing the variability of CWP in rice plots across the KVIS.

4. Discussion

Achieving the full potential of irrigated rice during the dry season through tailored soil and management practices is pivotal to the success of farming activities in the KVIS. In this study, soil physicochemical properties and plot characteristics affecting ET_a and CWP in irrigated rice in the KVIS were investigated. The spatial variation of ET_a and CWP (both obtained with PySEBAL) were predominantly linked to the distance between the plot and the irrigation scheme inlet, elevation, soil sand and silt contents, soil total nitrogen, and extractable potassium and zinc. Soil texture influences the movement of water in the soil, as well as its storage capacity and the amount of stored water that is available to the plants. The results from the linear mixed model showed negative relationships between ET_a and D_{PSI}, SL, SN, BLD, and positive relationships between ET_a and DtB, N and K contents. The negative relationships between ET_a and the sand or silt contents could be attributed to reduced soil water availability with an increase in sand and silt contents, leading to water stress and subsequent reduction in the ET_a by the rice plants (Haefele et al., 2006; Niang et al., 2018). The reduced ET_a with an increase in BLD could be related to reduced root growth due to higher soil compaction, which would limit the growth and development of the rice plants and result in reduced ET_a (Huang et al., 2012). We also noticed that soil water holding capacity and BLD were negatively correlated in this study (Fig. S1), and therefore, higher BLD is associated with lower soil water holding capacity, and higher water stress and reduced ET_a. Overall, soil texture and plot distance to the irrigation scheme inlet had great influences on the movement of water in the soil, as well as its storage capacity and the amount of stored water that is available to the plants. Therefore, practices that improved through for instance addition of organic matter have the potential to increase infiltration, water holding ability and actual evapotranspiration, and can be recommended to the farmers of the KVIS (Wilson et al., 2020).

There was a statistically significant and positive effect of soil nitrogen and potassium on ET_a in the KVIS during the study period. This can

Table 2
Estimates of fixed effects for PySEBAL-derived rice actual evapotranspiration (ET_a) and crop water productivity (CWP). Numbers in bold are those statistically significant. * and * * indicate a statistical significance at $\alpha = 0.05$ and $\alpha = 0.01$, respectively. *ns* denotes no statistical significance at $\alpha = 0.05$.

	ET_a	CWP
Intercept	**660.1** * *	**0.60** * *
Elv	3.0 ^{ns}	**-3.3 10^{-2}** * *
D_{PSI}	**-40.2** * *	**-2.6 10^{-2}** * *
DtB	**5.5** *	5.1 10^{-3} ^{ns}
SL	**-12.5** * *	4.3 10^{-3} ^{ns}
SN	**-7.3** *	4.4 10^{-3} ^{ns}
BLD	**-5.4** *	-5.3 10^{-4} ^{ns}
N	**20.8** * *	**-1.5 10^{-2}** *
K	**10.7** * *	-1.0 10^{-2} ^{ns}
pH	0.5 ^{ns}	-8.8 10^{-3} ^{ns}
Zn	-5.1 ^{ns}	-2.2 10^{-3} ^{ns}
Ca	1.1 ^{ns}	-4.5 10^{-3} ^{ns}
Fe	-0.4 ^{ns}	1.4 10^{-3} ^{ns}

Abbreviations: Elv: plot elevation; D_{PSI}: distance between plot and irrigation scheme inlet; DtB: depth to bedrock; Ca: soil extractable calcium; Fe: soil extractable iron; K: extractable potassium; N: soil total nitrogen; pH: potential of hydrogen; Zn: soil extractable zinc; BLD: bulk density; SL: silt content; SN: sand content.

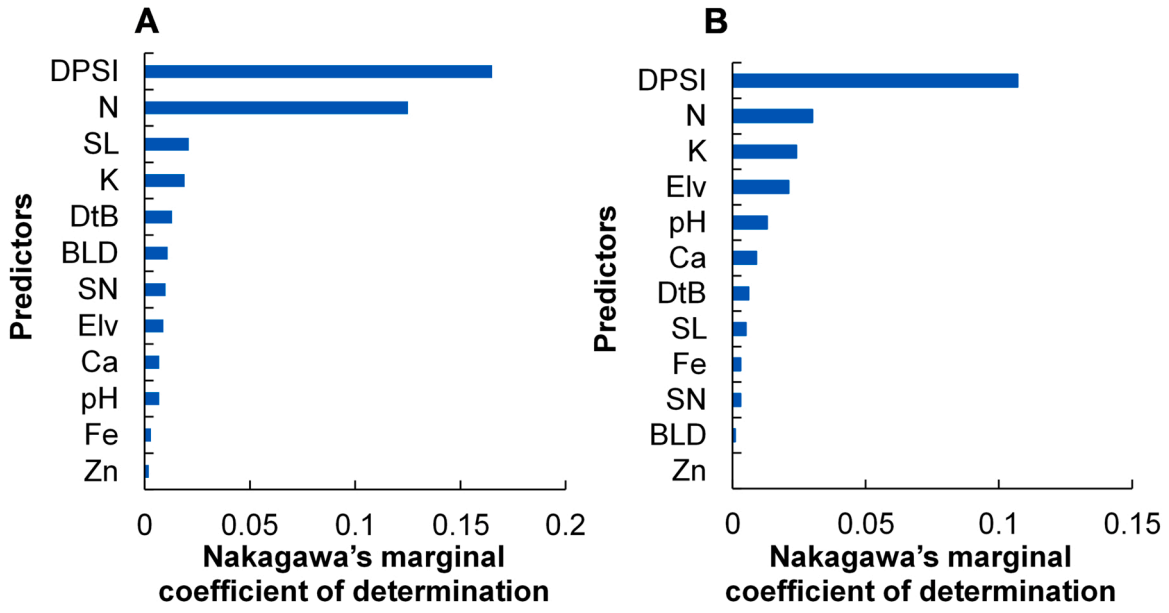

Fig. 3. Variable average contribution of each predictor in terms of the Nakagawa's marginal R^2 for rice actual evapotranspiration (**A**) and crop water productivity (**B**). Both rice actual evapotranspiration and crop water productivity were obtained using PySEBAL. Abbreviations: Elv: plot elevation; D_{PSI}: distance between the plot and the irrigation scheme inlet; DtB: depth to bedrock; Ca: soil extractable calcium; Fe: soil extractable iron; K: soil extractable potassium; N: soil total nitrogen; pH: potential of hydrogen; Zn: soil extractable zinc; BLD: bulk density; SL: silt content; SN: sand content.

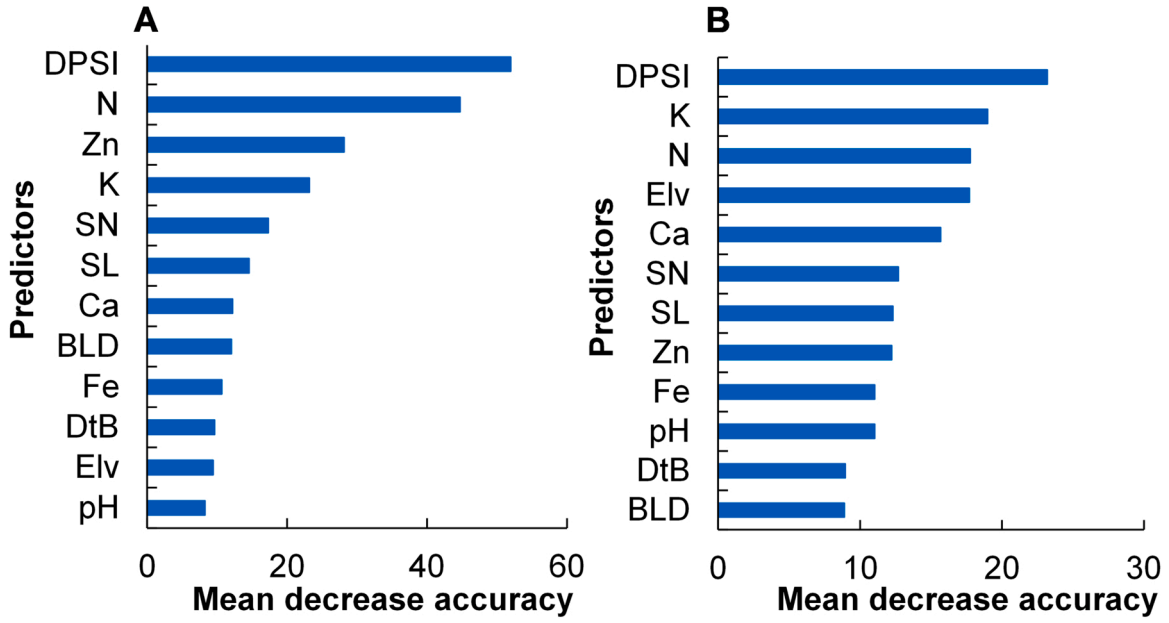

Fig. 4. Variable importance contribution in terms of mean decrease accuracy for rice actual evapotranspiration (**A**) and crop water productivity (**B**). Both rice actual evapotranspiration and crop water productivity were obtained using PySEBAL. Abbreviations: Elv: plot elevation; D_{PSI}: distance between the plot and the irrigation scheme inlet; DtB: depth to bedrock; Ca: soil extractable calcium; Fe: soil extractable iron; K: soil extractable potassium; N: soil total nitrogen; pH: potential of hydrogen; Zn: soil extractable zinc; BLD: bulk density; SL: silt content; SN: sand content.

be related to the role of both nutrients on photosynthesis and crop growth, which enhance the transpiration water loss, and result in higher ET_a (Skinner, 2013; Santos et al., 2016). Such results indicate that a good management of these two nutrients through soil fertility management remains crucial for the overall performance of the KVIS (Donovan et al., 1999; Dembelé et al., 2005; Yameogo et al., 2013). Supporting farmers in acquiring fertilizer, increase their awareness for best fertilizer management practices and strengthening their capacity in implementing integrated soil fertility management practices would help farmers in the KVIS effectively address the ongoing crop nutrients management issues (Wopereis et al., 1999; Wopereis and Defoer, 2007; Lompo et al., 2018).

The negative effect of the nitrogen on rice CWP, as shown in the LMM results, indicated that the proportional increase in ET_a due to the positive effect of the nitrogen is greater than the proportional increase in yield. Various factors including crop management practices, soil fertility, cropping calendars can influence CWP through their effects on ET_a and crop yield (Kijne and FAO, 2003; Nangia et al., 2008). Topography is well known as affecting CWP in rice (Bastiaanssen and Steduto, 2017; Foley et al., 2020; Dossou-Yovo et al., 2022). Our results indicate

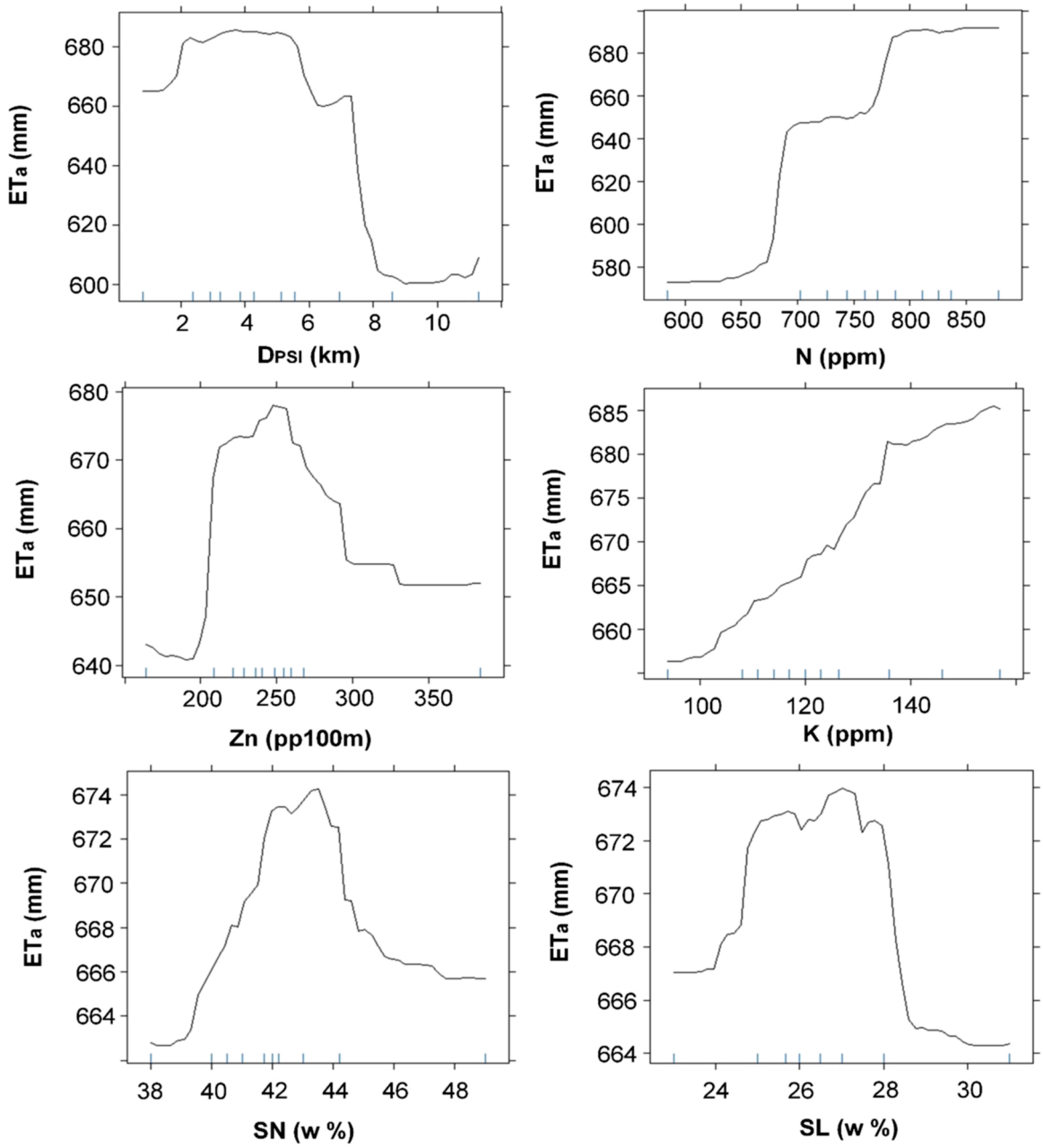

Fig. 5. Partial dependence plot of the six top predictors of PySEBAL-derived rice actual evapotranspiration (ET_a) based on random forest modeling. D_{PSI}: distance between the plot and the irrigation scheme inlet; N, Zn, K refer to soil total nitrogen, extractable zinc, and extractable potassium, respectively, and SN and SL soil contents in sand and silt, respectively.

that relatively lower CWP were found in irrigated plots located at higher altitudes in the KVIS, which can be related to soil erosion at these altitudes and the subsequent loss in soil fertility (Seibert et al., 2007; Karaca et al., 2018), indicating the need to improve land and soil water conservation at higher altitudes in the KVIS as reported in a previous study (Sawadogo et al., 2020b).

In basin irrigation systems, crop water productivity and actual evapotranspiration most often decrease as one moves away from the head of irrigation canals, given the reduced canal water supply (Van Dam et al., 2006; Latif, 2007). The distance between the plot and the scheme inlet (D_{PSI}) acted as the most influential factor for ET_a and CWP in our study for several reasons including the relatively high irrigation water consumption by head-enders compared to tail-enders in such irrigation schemes (Renault et al., 2013), and the poor water management of the KVIS. Indeed, the irrigation water management across the KVIS was carried out by inexperienced members of the Water Users Association, and that would probably affect more the tail-end farmers (Traoré, 2012; Wellens et al., 2013). Several studies reported that tail end farmers face challenges in having access to irrigation water when needed leading to water stress and yield penalty compared to farmers' fields located close to the water source (Sam-Amoah and Gowing, 2001; Zwart and Leclert, 2010). Training sessions and outputs from such studies are among the means used to improve the management of the KVIS. Growing crops with less water requirement in the tail of the scheme or using efficient irrigation systems such as drip irrigation system for the other crops grown in the KVIS can help improve the overall irrigation performance of the scheme.

Regarding the two modeling approaches used in the study, it has been shown that random forest-based models most often outperform multiple linear regression models (e.g. Breiman, 2001; Jeong et al.,

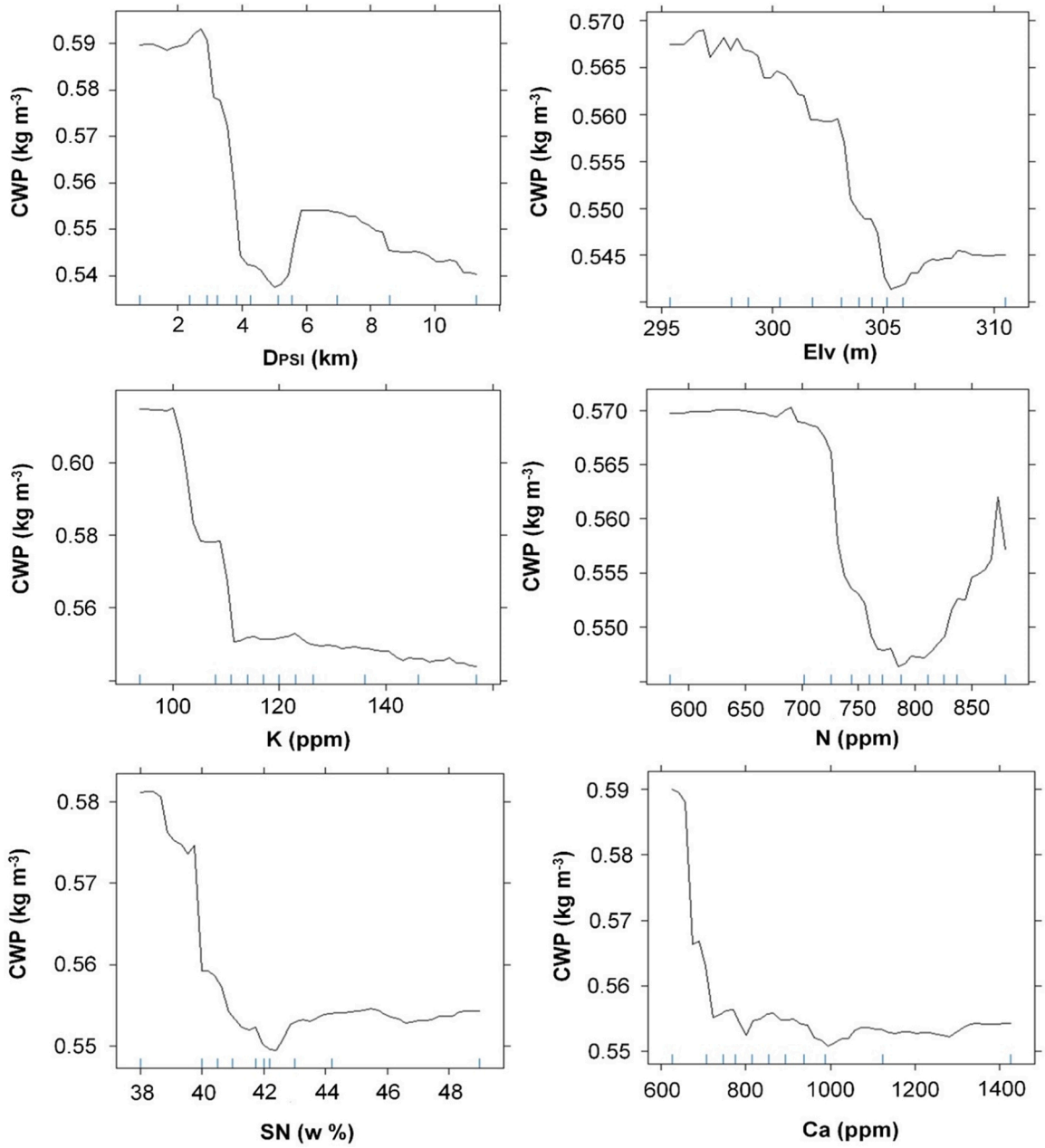

Fig. 6. Partial dependence plot of the six top predictors of PySEBAL-derived rice water productivity (CWP) based on random forest modeling. D_{PSI}: distance between the rice plot and the scheme inlet; Elv: plot elevation; N, K, and Ca refer to soil total nitrogen, extractable potassium, and extractable calcium, respectively, and SN soil content in sand.

2016). Our results were in line with such conclusions, at least for CWP (for ET_a both models resulted in similar performance). Jeong et al. (2016) argued that the relatively higher performance of RF-based models is likely more evident when the response is a result of complex interactions between multiple predictors, as it is the case in crop and farming systems and evidenced by the partial dependence plots (Figs. 5 and 6). Other factors such as vapor pressure deficit, water availability, crop variety, crop management practices, and socio-economic factors (e.g. water users association characteristics, proximity of farmers to the irrigation scheme, logistic challenges, etc.) can potentially impact on irrigation performance in irrigated perimeters and schemes (Zwart and Bastiaanssen, 2004; Dawe, 2005; Zhang et al., 2013). Including such potential variables would help improve our understanding of the key constraints of irrigation performance in the KVIS.

There were no experiments carried out to investigate the effect of each of the potential explanatory variables on ET_a and CWP in rice plots at the study site. Achieving this was beyond the scope of the study. Nevertheless, the effects of biophysical factors on crop evapotranspiration have already been documented (e.g. Allen et al., 1998; Katerji and Mastrorilli, 2009; Garrigues et al., 2015; Garrigues et al., 2018; Lehmann et al., 2018). Carrying out such experiments in the future could provide additional insights into developing better strategies to improve irrigation water management at the KVIS. Another limitation of the study was the short data period (two years). Expanding the data period to include several years with different climate patterns, improve the record keeping of the crop yield databases every season, and collect additional socio-economic data would improve the outcomes of the study. This is considered as part of a future potential research in the study country.

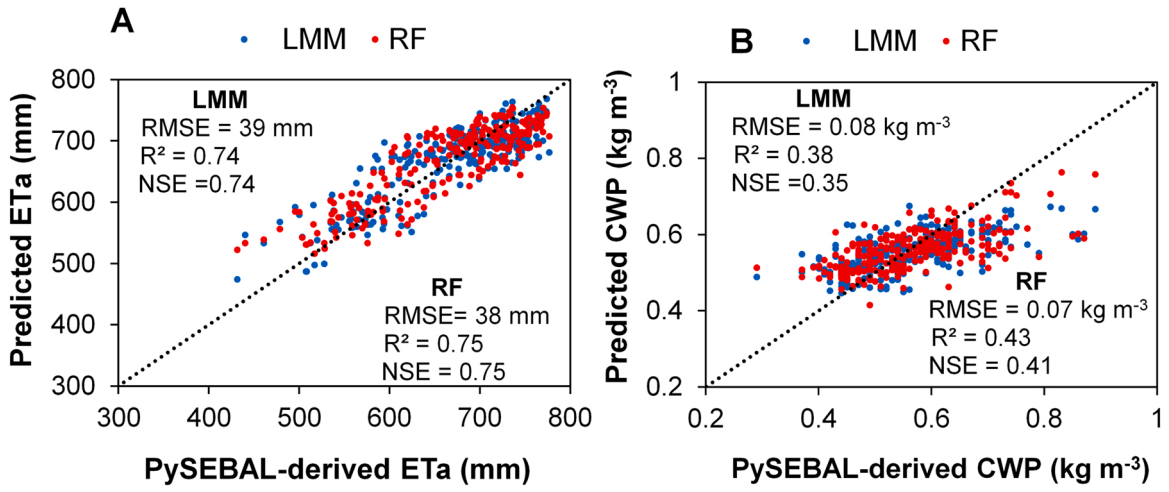

Fig. 7. Scatterplots of PySEBAL-derived versus predicted rice actual evapotranspiration (ET_a) (**A**), and crop water productivity (CWP) (**B**). Predicted values were obtained using linear mixed model (LMM) and random forest-based model (RF).

5. Conclusions

We investigated the potential soil physical and chemical properties and plot characteristics affecting the variability of irrigation performance in rice across the KVIS during the dry season production periods in 2013 and 2014 using two modeling approaches, random forest-based and linear mixed models. The main variables affecting rice ET_a and CWP (both obtained with PySEBAL) were the distance between plot and irrigation scheme inlet (D_{PSI}), plot elevation, soil content in sand and silt, soil total nitrogen, and soil extractable potassium and zinc. Various association patterns were found between ET_a or CWP and the top six predictors: non-monotonic association for all top six predictors in case of CWP, and either monotonic or non-monotonic association in case of ET_a depending on the predictor. Results also indicated that relatively good-performing rice plots in terms of CWP were those located close to the scheme perimeter and at relatively lower altitudes in the KVIS. The effects of soil nitrogen and potassium on ET_a and CWP in rice across the irrigation scheme suggest that good soil fertility management would be beneficial to rice. Both LMM and RF-based models achieved good performance in predicting ET_a: The fair models' performances for predicting CWP (NSE for LMM and RF being 0.35 and 0.41, respectively; and corresponding RMSE of 0.08 kg m^{-3} and 0.07 kg m^{-3}) indicate that additional observational data might be needed to improve our understanding of the key constraints of irrigation performance in the KVIS. Nonetheless, this study can serve as a basis for improving irrigation water management through helping the KVIS managers to strategically locate underperforming plots to better prioritize their operations. Future research to improve our understanding of the key constraints of irrigation performance in the KVIS can include investigating potential factors influencing irrigation performance such as water availability, demographics of irrigation water users, households' characteristics, proximity of farmers to the irrigation scheme, logistic challenges, credit accessibility, and other crop management practices (e.g. weed, pests and diseases management, transplanting dates, and water management practices), in addition to remote sensing-derived information.

Declaration of Competing Interest

The authors declare that they have no known competing financial interests or personal relationships that could have appeared to influence the work reported in this paper.

Data availability

Data will be made available on request.

Acknowledgments

The first author was supported by the Presidency for Turks Abroad and Related Communities (YTB) fund. We are grateful to the managers of the Kou Valley irrigation scheme, particularly Mr. Lassané Kaboré for sharing the crop yield and management data.

Appendix A. Supporting information

Supplementary data associated with this article can be found in the online version at doi:10.1016/j.agwat.2022.108124.

References

Ahmad, M.D., Turral, H., Nazeer, A., 2009. Diagnosing irrigation performance and water productivity through satellite remote sensing and secondary data in a large irrigation system of Pakistan. Agr. Water Manag. 96, 551–564. https://doi.org/10.1016/j.agwat.2008.09.017.

Akpoti, K., Kabo-bah, A.T., Dossou-Yovo, E.R., Groen, T.A., Zwart, S.J., 2020. Mapping suitability for rice production in inland valley landscapes in Benin and Togo using environmental niche modeling. Sci. Total Environ. 709, 136165 https://doi.org/10.1016/j.scitotenv.2019.136165.

Akpoti, K., Groen, T., Dossou-Yovo, E., Kabo-bah, A.T., Zwart, S.J., 2022. Climate change-induced reduction in agricultural land suitability of West-Africa's inland valley landscapes. Agr. Syst. 200, 103429 https://doi.org/10.1016/j.agsy.2022.103429.

Allen, R.G., Pereira, L.S., Raes, D., Smith, M., 1998, Crop evapotranspiration: Guidelines for computing crop water requirements. FAO Irrigation and Drainage Paper 56. Food and Agriculture Organization of the United Nations (FAO), https://www.fao.org/3/x0490e/x0490e00.htm (accessed 20 October 2022).

United Nations, 2015, Transforming our world: the 2030 Agenda for Sustainable Development. Resolution adopted by the General Assembly on 25 September 2015. Washington, D.C., USA. ⟨https://sustainabledevelopment.un.org/content/documents/21252030%20Agenda%20for%20Sustainable%20Development%20web.pdf⟩ (accessed 20 October 2022).

Azen, R., Budescu, D.V., 2003. The dominance analysis approach for comparing predictors in multiple regression. Psychol. Methods 8, 129–148. https://doi.org/10.1037/1082-989X.8.2.129.

Bastiaanssen, W.G.M., Ali, S., 2003. A new crop yield forecasting model based on satellite measurements applied across the Indus Basin, Pakistan. Agr. Ecosyst. Environ. 94, 321–340. https://doi.org/10.1016/S0167-8809(02)00034-8.

Bastiaanssen, W.G.M., Bos, M.G., 1999. Irrigation performance indicators based on remotely sensed data: a review of literature. Irrig. Drain. Syst. 13, 291–311. https://doi.org/10.1023/A:1006355315251.

Bastiaanssen, W.G.M., Steduto, P., 2017. The water productivity score (WPS) at global and regional level: Methodology and first results from remote sensing measurements of wheat, rice and maize. Sci. Total Environ. 575, 595–611. https://doi.org/10.1016/j.scitotenv.2016.09.032.

Bastiaanssen, W.G.M., Noordman, E.J.M., Pelgrum, H., Davids, G., Thoreson, B.P., Allen, R.G., 2005. SEBAL model with remotely sensed data to improve water-resources management under actual field conditions. J. Irrig. Drain. Eng. 131, 85–93. https://doi.org/10.1061/(ASCE)0733-9437(2005)131:1(85).

Bates, D., Mächler, M., Bolker, B., Walker, S., 2015, lme4: Linear Mixed-Effects Models Using Eigen and S4. (R package version 1.1–10). ⟨https://CRAN.R-project.org/package=lme4⟩.

Blatchford, M.L., Mannaerts, C.M., Zeng, Y., Nouri, H., Karimi, P., 2019. Status of accuracy in remotely sensed and in-situ agricultural water productivity estimates: A review. Remote Sens. Environ. 234, 111413 https://doi.org/10.1016/j.rse.2019.111413.

Bos, M.G., Burton, M.A., Molden, D.J., 2005. Irrigation and drainage performance assessment: practical guidelines. CABI Pub,, Wallingford.

Breiman, L., 2001. Random Forests. Mach. Learn. 45, 5–32. https://doi.org/10.1023/A:1010933404324.

Bustos-Navarrete, C., Filipa, C.S., 2020, Dominance analysis for general, generalized and mixed linear models. (R package version 2.0.0). ⟨https://CRAN.R-project.org/package=dominanceanalysis⟩.

Chang, D.-H., Islam, S., 2000. Estimation of soil physical properties using remote sensing and artificial neural network. Remote Sens. Environ. 74, 534–544. https://doi.org/10.1016/S0034-4257(00)00144-9.

Cutler, D.R., Edwards Jr., T.C., Beard, K.H., Cutler, A., Hess, K.T., Gibson, J., Lawler, J.J., 2007. Random forests for classification in ecology. Ecology 88, 2783–2792. https://doi.org/10.1890/07-0539.1.

Dawe, D., 2005. Increasing water productivity in rice-based systems in Asia – past trends, current problems, and future prospects. Plant Prod. Sci. 8, 221–230. https://doi.org/10.1626/pps.8.221.

Dembelé, Y., Kambiré, H., Sié, M., 2005. Gestion de l'eau et de l'azote en riziculture irriguée au Burkina Faso. Cah. Agr. 14, 569–572.

Dembélé, Y., Yacouba, H., Keïta, A., Sally, H., 2012. Assessment of irrigation system performance in south-western Burkina Faso. Irrig. Drain. 61, 306–315. https://doi.org/10.1002/ird.647.

Djagba, J.F., Sintondji, L.O., Kouyaté, A.M., Baggie, I., Agbahungba, G., Hamadoun, A., Zwart, S.J., 2018. Predictors determining the potential of inland valleys for rice production development in West Africa. Appl. Geogr. 96, 86–97. https://doi.org/10.1016/j.apgeog.2018.05.003.

Donovan, C., Wopereis, M.C.S., Guindo, D., Nebié, B., 1999. Soil fertility management in irrigated rice systems in the Sahel and Savanna regions of West Africa: Part II. Profitability and risk analysis. Field Crops Res 61, 147–162. https://doi.org/10.1016/S0378-4290(98)00153-1.

Dossou-Yovo, E.R., Zwart, S.J., Kouyaté, A., Ouédraogo, I., Bakare, O., 2019. Predictors of drought in inland valley landscapes and enabling factors for rice farmers' mitigation measures in the Sudan-Sahel zone. Sustainability 11, 79. https://doi.org/10.3390/su11010079.

Dossou-Yovo, E.R., Devkota, K.P., Akpoti, K., Danvi, A., Duku, C., Zwart, S.J., 2022. Thirty years of water management research for rice in sub-Saharan Africa: Achievement and perspectives. Field Crops Res 283, 108548. https://doi.org/10.1016/j.fcr.2022.108548.

DRASA-Ouest, 2014, Production saisonnière sur la plaine de la Vallée du Kou de 2008 à 2014. Direction régionale de l'agriculture et de la sécurité alimentaire (DRASA), Ouagadougou, Burkina Faso.

ESRI, 2016, Arcgis desktop: Release 10. Environmental Systems Research Institute (ESRI), ⟨https://www.esri.com/en-us/home⟩.

FAO, 2020, FAOSTAT database. Food and Agriculture Organization of the United Nations (FAO). ⟨http://www.fao.org/faostat/en/#home⟩ (accessed 20 October 2022).

Farr, T.G., Rosen, P.A., Caro, E., Crippen, R., Duren, R., Hensley, S., Kobrick, M., Paller, M., Rodriguez, E., Roth, L., Seal, D., Shaffer, S., Shimada, J., Umland, J., Werner, M., Oskin, M., Burbank, D., Alsdorf, D., 2007. The Shuttle Radar Topography Mission. Rev. Geophys. 45. https://doi.org/10.1029/2005RG000183.

Foley, D.J., Thenkabail, P.S., Aneece, I.P., Teluguntla, P.G., Oliphant, A.J., 2020. A meta-analysis of global crop water productivity of three leading world crops (wheat, corn, and rice) in the irrigated areas over three decades. Int. J. Digit. Earth 13, 939–975. https://doi.org/10.1080/17538947.2019.1651912.

Fontanet, M., Fernàndez-Garcia, D., Ferrer, F., 2018. The value of satellite remote sensing soil moisture data and the DISPATCH algorithm in irrigation fields. Hydrol. Earth Syst. Sci. 22, 5889–5900. https://doi.org/10.5194/hess-22-5889-2018.

Forkuor, G., Hounkpatin, O.K.L., Welp, G., Thiel, M., 2017. High resolution mapping of soil properties using remote sensing variables in south-western Burkina Faso: A comparison of machine learning and multiple linear regression models. PLOS ONE 12, e0170478. https://doi.org/10.1371/journal.pone.0170478.

Friedman, J.H., 2001. Greedy function approximation: A gradient boosting machine. Ann. Stat. 1189–1232.

Garrigues, S., Olioso, A., Calvet, J.C., Martin, E., Lafont, S., Moulin, S., Chanzy, A., Marloie, O., Buis, S., Desfonds, V., Bertrand, N., Renard, D., 2015. Evaluation of land surface model simulations of evapotranspiration over a 12-year crop succession: impact of soil hydraulic and vegetation properties. Hydrol. Earth Syst. Sci. 19, 3109–3131. https://doi.org/10.5194/hess-19-3109-2015.

Garrigues, S., Boone, A., Decharme, B., Olioso, A., Albergel, C., Calvet, J.C., Moulin, S., Buis, S., Martin, E., 2018. Impacts of the soil water transfer parameterization on the simulation of evapotranspiration over a 14-year mediterranean crop succession. J. Hydrometeorol. 19, 3–25. https://doi.org/10.1175/JHM-D-17-0058.1.

Ge, Y., Thomasson, J.A., Sui, R., 2011. Remote sensing of soil properties in precision agriculture: A review. Front. Earth Sci. 5, 229–238. https://doi.org/10.1007/s11707-011-0175-0.

Gelman, A., Hill, J., 2007. Data Analysis Using Regression and Multilevel/hierarchical Models. Cambridge University Press,, New York.

Haefele, S.M., Naklang, K., Harnpichitvitaya, D., Jearakongman, S., Skulkhu, E., Romyen, P., Phasopa, S., Tabtim, S., Suriya-arunroj, D., Khunthasuvon, S., Kraisorakul, D., Youngsuk, P., Amarante, S.T., Wade, L.J., 2006. Factors affecting rice yield and fertilizer response in rainfed lowlands of northeast Thailand. Field Crops Res 98, 39–51. https://doi.org/10.1016/j.fcr.2005.12.003.

Hengl, T., Heuvelink, G.B.M., Kempen, B., Leenaars, J.G.B., Walsh, M.G., Shepherd, K.D., Sila, A., MacMillan, R.A., Mendes de Jesus, J., Tamene, L., Tondoh, J.E., 2015. Mapping soil properties of Africa at 250 m resolution: Random forests significantly improve current predictions. PLOS ONE 10, e0125814. https://doi.org/10.1371/journal.pone.0125814.

Hengl, T., Leenaars, J.G.B., Shepherd, K.D., Walsh, M.G., Heuvelink, G.B.M., Mamo, T., Tilahun, H., Berkhout, E., Cooper, M., Fegraus, E., Wheeler, I., Kwabena, N.A., 2017. Soil nutrient maps of Sub-Saharan Africa: assessment of soil nutrient content at 250 m spatial resolution using machine learning. Nut. Cyc. Agroecosys 109, 77–102. https://doi.org/10.1007/s10705-017-9870-x.

Huang, M., Zou, Y., Jiang, P., Xia, B., Feng, Y., Cheng, Z., Mo, Y., 2012. Effect of tillage on soil and crop properties of wet-seeded flooded rice. Field Crops Res 129, 28–38. https://doi.org/10.1016/j.fcr.2012.01.013.

ISRIC, 2014, Africa Soil Profiles Database, version 1.2. International Soil Reference and Information Centre (ISRIC) - World Soil Information. ⟨https://files.isric.org/public/afsp/AF-AfSP1.2.zip⟩.

Jeong, J.H., Resop, J.P., Mueller, N.D., Fleisher, D.H., Yun, K., Butler, E.E., Timlin, D.J., Shim, K.-M., Gerber, J.S., Reddy, V.R., Kim, S.-H., 2016. Random forests for global and regional crop yield predictions. PLOS ONE 11, e0156571. https://doi.org/10.1371/journal.pone.0156571.

Karaca, S., Gülser, F., Selçuk, R., 2018. Relationships between soil properties, topography and land use in the Van Lake Basin, Turkey. Eurasia J. Soil Sci. 7, 115–120. https://doi.org/10.18393/ejss.348412.

Katerji, N., Mastrorilli, M., 2009. The effect of soil texture on the water use efficiency of irrigated crops: Results of a multi-year experiment carried out in the Mediterranean region. Eur. J. Agron. 30, 95–100. https://doi.org/10.1016/j.eja.2008.07.009.

Kharrou, M.H., Le Page, M., Chehbouni, A., Simonneaux, V., Er-Raki, S., Jarlan, L., Ouzine, L., Khabba, S., Chehbouni, G., 2013. Assessment of equity and adequacy of water delivery in irrigation systems using remote sensing-based indicators in semi-arid region, Morocco. Water Res. Manag. 27, 4697–4714. https://doi.org/10.1007/s11269-013-0438-5.

Kijne, J.W., FAO, 2003, Unlocking the water potential of agriculture. Food and Agriculture Organization of the United Nations (FAO), Rome. ⟨https://www.fao.org/3/Y4525E/y4525e00.htm⟩ (accessed 20 October 2022).

Kouadio, L., Deo, R.C., Byrareddy, V., Adamowski, J.F., Mushtaq, S., Nguyen, V.P., 2018. Artificial intelligence approach for the prediction of Robusta coffee yield using soil fertility properties. Comp. Electron. Agr. 155, 324–338. https://doi.org/10.1016/j.compag.2018.10.014.

Kuhn, M., Wing, J., Weston, S., Williams, A., Keefer, C., Engelhardt, A., Cooper, T., Mayer, Z., Kenkel, B., R. Core Team, 2020, caret: Classification and Regression Training. (R package version 6.0–86). ⟨https://CRAN.R-project.org/package=caret⟩.

Laborte, A.G., Maunahan, A.A., Hijmans, R.J., 2012. Opportunities for expanding paddy rice production in Laos: spatial predictive modeling using Random Forest. J. Land Use Sci. 7, 21–33. https://doi.org/10.1080/1747423X.2010.519788.

Laird, N.M., Ware, J.H., 1982. Random-effects models for longitudinal data. Biometrics 38, 963–974. https://doi.org/10.2307/2529876.

Latif, M., 2007. Spatial productivity along a canal irrigation system in Pakistan. Irrig. Drain. 56, 509–521. https://doi.org/10.1002/ird.320.

Lebel, T., Ali, A., 2009. Recent trends in the Central and Western Sahel rainfall regime (1990–2007). J. Hydrol. 375, 52–64. https://doi.org/10.1016/j.jhydrol.2008.11.030.

Leenaars, J., Van Oostrum, A., Ruiperez Gonzalez, M., 2014, Africa soil profiles database version 1.2. A compilation of georeferenced and standardized legacy soil profile data for Sub-Saharan Africa (with dataset). ISRIC Report 2014/01. ISRIC–World Soil Information, Wageningen. p. 162. ⟨https://edepot.wur.nl/481288⟩ (accessed 20 October 2022).

Lehmann, P., Merlin, O., Gentine, P., Or, D., 2018. Soil texture effects on surface resistance to bare-soil evaporation, 398-310, 405 Geophys. Res. Lett. 45 (10). https://doi.org/10.1029/2018GL078803.

Liaw, A., Wiener, M., 2002. Classification and regression by randomForest. R. N. 2, 18–22.

Liaw, A., Wiener, M., 2018, randomForest: Breiman and Cutler's Random Forests for Classification and Regression. (R package version 4.6–14). ⟨https://CRAN.R-project.org/package=randomForest⟩.

Lompo, F., Bationo, A., Sedogo, M.P., Bado, V.B., Hien, V., Ouattara, B., 2018. Role of Local Agro-minerals in Mineral Fertilizer Recommandations for Crops: Examples of Some West Africa Phosphate Rocks. In: Bationo, A., Ngaradoum, D., Youl, S., Lompo, F., Fening, J.O. (Eds.), Improving the Profitability, Sustainability and Efficiency of Nutrients Through Site Specific Fertilizer Recommendations in West Africa Agro-Ecosystems, Volume 1. Springer International Publishing, Cham, pp. 157–180.

Luo, W., Azen, R., 2013. Determining predictor importance in hierarchical linear models using dominance analysis. In: J. Educ. Behav. Stat, 38, pp. 3–31. https://doi.org/10.3102/1076998612458319.

Mellor, A., Haywood, A., Stone, C., Jones, S., 2013. The performance of random forests in an operational setting for large area sclerophyll forest classification. In: Remote Sens, 5, pp. 2838–2856. https://doi.org/10.3390/rs5062838.

Mohamed, E.S., Ali, A., El-Shirbeny, M., Abutaleb, K., Shaddad, S.M., 2019. Mapping soil moisture and their correlation with crop pattern using remotely sensed data in arid region. Egyp. J. Remote Sens. Space Sci. https://doi.org/10.1016/j.ejrs.2019.04.003.

Nakagawa, S., Schielzeth, H., 2013. A general and simple method for obtaining R2 from generalized linear mixed-effects models. Meth. Ecol. Evol. 4, 133–142. https://doi.org/10.1111/j.2041-210x.2012.00261.x.

Nangia, V., Turral, H., Molden, D., 2008. Increasing water productivity with improved N fertilizer management. Irrig. Drain. Syst. 22, 193–207. https://doi.org/10.1007/s10795-008-9051-9.

Niang, A., Becker, M., Ewert, F., Tanaka, A., Dieng, I., Saito, K., 2018. Yield variation of rainfed rice as affected by field water availability and N fertilizer use in central Benin. Nutr. Cycl. Agroecosyst. 110, 293–305. https://doi.org/10.1007/s10705-017-9898-y.

Nishikawa, T., Li, K., Inamura, T., 2014. Nitrogen uptake by the rice plant and changes in the soil chemical properties in the paddy rice field during yearly application of anaerobically-digested manure for seven years. Plant Prod. Sci. 17, 237–244. https://doi.org/10.1626/pps.17.237.

Nitcheu, M., Midékor, A., Sawadogo, B., 2014, Restitution des travaux de suivi de la campagne saison sèche 2014 sur le périmètre rizicole de la vallée du Kou. AEDE/OE, Bobo-Dioulasso, Burkina Faso.

Paturel, J.E., Boubacar, I., L'Aour, A., Mahé, G., 2010. Analyses de grilles pluviométriques et principaux traits des changements survenus au 20ème siècle en Afrique de l'Ouest et Centrale. Hydrol. Sci. J. 55, 1281–1289. https://doi.org/10.1080/02626667.2010.527846.

Peng, H., Lu, Y., 2012. Model selection in linear mixed effect models. J. Multivar. Anal. 109, 109–129. https://doi.org/10.1016/j.jmva.2012.02.005.

Pinheiro, J., Bates, D., DebRoy, S., Sarkar, D., R Core Team, 2020, nlme: Linear and Nonlinear Mixed Effects Models. (Version 3.1–147). ⟨https://CRAN.R-project.org/package=nlme⟩.

Prasad, A.M., Iverson, L.R., Liaw, A., 2006. Newer classification and regression tree techniques: Bagging and random forests for ecological prediction. Ecosystems 9, 181–199. https://doi.org/10.1007/s10021-005-0054-1.

R Core Team, 2020, R: A language and environment for statistical computing. Vienna, Austria. ⟨https://www.r-project.org/⟩.

Renault, D., Wahaj, R., Smits, S., 2013, Multiple uses of water services in large irrigation systems - Auditing and planning modernization - The MASSMUS Approach. FAO Irrigation and Drainage Paper 67. Food and Agriculture Organization of the United Nations (FAO), Rome, Italy. ⟨https://www.fao.org/3/i3414e/i3414e.pdf⟩ (accessed 20 October 2022).

Sam-Amoah, L.K., Gowing, J.W., 2001. Assessing the performance of irrigation schemes with minimum data on water deliveries1. Irrig. Drain. 50, 31–39. https://doi.org/10.1002/ird.12.

Santos, A.Bd, Fageria, N.K., Stone, L.F., Santos, T.P.B., 2016. Effect of irrigation and nitrogen fertilization on the agronomic traits and yield of irrigated rice. Rev. Ceres 63, 724–731. https://doi.org/10.1590/0034-737x201663050018.

Sawadogo, A., Hessels, T., Gündoğdu, K.S., Demir, A.O., Mustafa, Ü., Zwart, S.J., 2020a. Comparative analysis of the PySEBAL model and lysimeter for estimating actual evapotranspiration of soybean crop in Adana, Turkey. Int. J. Eng. Geosci. 5, 60–65. https://doi.org/10.26833/ijeg.573503.

Sawadogo, A., Kouadio, L., Traoré, F., Zwart, S.J., Hessels, T., Gündoğdu, K.S., 2020b. Spatiotemporal assessment of irrigation performance of the Kou Valley irrigation scheme in Burkina Faso using satellite remote sensing-derived indicators. ISPRS Int. J. Geo-Inf. 9, 484. https://doi.org/10.3390/ijgi9080484.

Seibert, J., Stendahl, J., Sørensen, R., 2007. Topographical influences on soil properties in boreal forests. Geoderma 141, 139–148. https://doi.org/10.1016/j.geoderma.2007.05.013.

Sheffield, K., Morse-McNabb, E., 2015. Using satellite imagery to asses trends in soil and crop productivity across landscapes. IOP Conf. Ser. Earth Environ. Sci. 25, 012013. doi: 10.1088/1755–1315/25/1/012013.

Skinner, R.H., 2013. Nitrogen fertilization effects on pasture photosynthesis, respiration, and ecosystem carbon content. Agr. Ecosys. Environ. 172, 35–41. https://doi.org/10.1016/j.agee.2013.04.005.

Steduto, P., Hsiao, C.T., Fereres, E., Raes, D., 2012, Crop yield response to water. FAO Irrigation and Drainage Paper No. 66. Food and Agriculture Organization of the United Nations (FAO), Rome, Italy. ⟨https://www.fao.org/3/i2800e/i2800e.pdf⟩ (accessed 20 October 2022).

Traoré, F., 2012, Optimisation de l'utilisation des ressources en eau du bassin du Kou pour des usages agricoles. Ph.D. Thesis. Université de Liège, Liège, Belgium. ⟨https://hdl.handle.net/2268/132698⟩.

UNDESAPD, 2014, World Urbanization Prospects: The 2014 Revision, Highlights (ST/ESA/SER.A/352). United Nations, New York, NY, U.S.A. ⟨https://www.compassion.com/multimedia/world-urbanization-prospects.pdf⟩ (accessed 20 October 2022).

UN-Water, 2018, The United Nations World Water Development Report 2018: Nature-Based Solutions for Water. UNESCO, Paris, France. ⟨https://unesdoc.unesco.org/ark:/48223/pf0000261424⟩ (accessed 20 October 2022).

Van Dam, J.C., Singh, R., Bessembinder, J.J.E., Leffelaar, P.A., Bastiaanssen, W.G.M., Jhorar, R.K., Kroes, J.G., Droogers, P., 2006. Assessing options to increase water productivity in irrigated river basins using remote sensing and modelling tools. Int. J. Water Res. Dev. 22, 115–133. https://doi.org/10.1080/07900620500405734.

Wellens, J., Compaoré, N.F., Van Orshoven, J., Raes, D., Yacouba, H., Ouattara, A., 2004, Renforcement de la capacité de gestion des ressources en eau dans l'agriculture moyennant des outils de suivi-évaluation (Burkina Faso): Rapport Technique. ⟨https://orbi.uliege.be/handle/2268/172111⟩ (accessed 20 October 2022).

Wellens, J., Nitcheu, M., Traore, F., Tychon, B., 2013. A public–private partnership experience in the management of an irrigation scheme using decision-support tools in Burkina Faso. Agr. Water Manag. 116, 1–11. https://doi.org/10.1016/j.agwat.2012.09.013.

Wilson, T.G., Kustas, W.P., Alfieri, J.G., Anderson, M.C., Gao, F., Prueger, J.H., McKee, L.G., Alsina, M.M., Sanchez, L.A., Alstad, K.P., 2020. Relationships between soil water content, evapotranspiration, and irrigation measurements in a California drip-irrigated Pinot noir vineyard. Agr. Water Manag. 237, 106186 https://doi.org/10.1016/j.agwat.2020.106186.

Wopereis, M.C.S., Defoer, T., 2007. Moving methodologies to enhance agricultural productivity of rice-based lowland systems in sub-Saharan Africa. In: Bationo, A., Waswa, B., Kihara, J., Kimetu, J. (Eds.), Advances in Integrated Soil Fertility Management in sub-Saharan Africa: Challenges and Opportunities. Springer Netherlands, Dordrecht, pp. 1077–1091.

Wopereis, M.C.S., Donovan, C., Nebié, B., Guindo, D., N'Diaye, M.K., 1999. Soil fertility management in irrigated rice systems in the Sahel and Savanna regions of West Africa: Part I. Agronomic analysis. Field Crops Res 61, 125–145. https://doi.org/10.1016/S0378-4290(98)00154-3.

Yameogo, P., Segde, Z., Dakouo, D., Sedogo, M., 2013. Placement profond de l'urée (PPU) et amélioration de l'efficacité d'utilisation de l'azote en riziculture irriguée dans le périmètre rizicole de Karfiguela au Burkina Faso. J. Appl. Biosci. 70, 5523–5530. https://doi.org/10.4314/jab.v70i1.98749.

Yu, T.R., 1991, Characteristics of soil acidity of paddy soils in relation to rice growth, in: Wright, R.J., Baligar, V.C., Murrmann, R.P. (Eds.), Plant-Soil Interactions at Low pH: Proceedings of the Second International Symposium on Plant-Soil Interactions at Low pH, 24–29 June 1990, Beckley West Virginia, USA. Springer Netherlands, Dordrecht, pp. 107–112.

Yuzugullu, O., Lorenz, F., Fröhlich, P., Liebisch, F., 2020. Understanding fields by remote sensing: Soil zoning and property mapping. Remote Sens 12, 1116. https://doi.org/10.3390/rs12071116.

Zhang, L., Heerink, N., Dries, L., Shi, X., 2013. Water users associations and irrigation water productivity in northern China. Ecol. Econ. 95, 128–136. https://doi.org/10.1016/j.ecolecon.2013.08.014.

Zwart, S.J., Bastiaanssen, W.G.M., 2004. Review of measured crop water productivity values for irrigated wheat, rice, cotton and maize. Agr. Water Manag. 69, 115–133. https://doi.org/10.1016/j.agwat.2004.04.007.

Zwart, S.J., Bastiaanssen, W.G.M., 2007. SEBAL for detecting spatial variation of water productivity and scope for improvement in eight irrigated wheat systems. Agr. Water Manag. 89, 287–296. https://doi.org/10.1016/j.agwat.2007.02.002.

Zwart, S.J., Leclert, L.M.C., 2010. A remote sensing-based irrigation performance assessment: a case study of the Office du Niger in Mali. Irrig. Sci. 28, 371–385. https://doi.org/10.1007/s00271-009-0199-3.